The University of Osaka
Institutional Knowledge Archive

Atomic-scale flattening of SiC surfaces by electroless chemical etching in HF solution with Pt catalyst

Kenta Arima,[a)] Hideyuki Hara, and Junji Murata
Department of Precision Science and Technology, Graduate School of Engineering, Osaka University, 2-1, Yamada-oka, Suita, Osaka 565-0871, Japan

Takeshi Ishida, Ryota Okamoto, and Keita Yagi
Research Center for Ultra-Precision Science and Technology, Graduate School of Engineering, Osaka University, 2-1, Yamada-oka, Suita, Osaka 565-0871, Japan

Yasuhisa Sano, Hidekazu Mimura, and Kazuto Yamauchi
Department of Precision Science and Technology, Graduate School of Engineering, Osaka University, 2-1, Yamada-oka, Suita, Osaka 565-0871, Japan
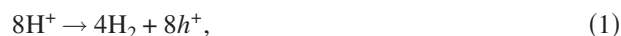
The authors present a method for flattening SiC surfaces with Pt as a catalyst in HF solution. The mechanism for flattening SiC surfaces is discussed. The flattened $4H$-SiC(0001) surface is composed of alternating wide and narrow terraces with single-bilayer-height steps, which are induced by the rate difference of the catalytic reactions between adjacent terraces. Scanning tunneling microscopy images reveal a 1×1 phase on the terraces. The 1×1 phase is composed of coexisting of F- and OH-terminated Si atoms, which originate from the polarization of the underlying Si–C bonds. © *2007 American Institute of Physics*. [DOI: 10.1063/1.2739084]

Silicon carbide (SiC) is a representative hard material with a Knoop hardness of 24.5–31.4 GPa.[1] Recently, the surface flattening of SiC has attracted a great deal of attention for the following reasons. SiC is a promising wide-band-gap semiconductor for electronic devices operated under extreme conditions such as high power and high temperature because of its excellent electronic properties such as high thermal conductivity and high breakdown field. In analogy with Si electronics, the preparation of clean, flat, and well-ordered SiC surfaces is important for the fabrication of SiC-based devices with high performance.[2] However, conventional flattening processes are not effective for SiC surfaces because of high strength and chemical inertness of SiC. For example, mechanical polishing with diamond abrasives leaves disordered layers on the SiC surface. Wet-chemical treatments using alkaline (KOH) or acid (HF) solutions remove the disordered layers, but the obtained surface is far from being atomically flat.[3] Only treatments at elevated temperatures in ultrahigh vacuum (UHV) create clean and reconstructed SiC surfaces.[3–5] However, a large amount of energy consumption is necessary to reconstruct an entire inch-scaled wafer surface. We have found that the use of a Pt plate as a catalyst is effective for flattening SiC surfaces in HF solution.[6] In this letter, we present the mechanism of the flattening process, and the flattening performance is evaluated on the atomic scale by scanning probe microscopy.
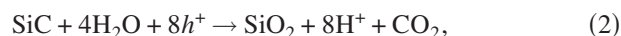
It has been reported that the etching of semiconductors in HF-based solutions is enhanced by the presence of some noble metals. In these processes, H_2O_2, Fe(III) ions, $K_2S_2O_8$, protons, or oxygen, which are included in the solutions, are catalytically reduced on the surface of noble metals.[7–12] The created holes subsequently participate in the oxidation and dissolution of the semiconductor surfaces. These etching processes have been applied for the fabrication of nanoholes on the surfaces or porous surfaces. To utilize these chemical

reactions for the flattening of SiC surfaces, an unpolished n-type $4H$-SiC(0001) wafer (0.02–0.03 Ω cm) was placed on a Pt plate with a controlled pressure of 0.02 MPa in concentrated HF solution (50%). Both the Pt plate and the SiC sample were rotated independently in the same plane. We propose that electroless etching occurs at contact sites of the SiC surface with Pt by the following mechanism.

For cathode (Pt),

$$8H^+ \rightarrow 4H_2 + 8h^+, \tag{1}$$

and for anode (SiC),

$$SiC + 4H_2O + 8h^+ \rightarrow SiO_2 + 8H^+ + CO_2, \tag{2}$$

$$SiO_2 + 6HF \rightarrow H_2SiF_6 + 2H_2O. \tag{3}$$

Assuming that the Pt surface is flat, only protrusions or microbumps on the SiC surface are in contact with the Pt catalyst. The holes, formed as shown in Eq. (1), are injected into the valence band of the protrusions on SiC, and these protrusions are removed by the chemical reactions shown in Eqs. (2) and (3) As a result, the SiC surface is flattened. The dissolved oxygen in HF solution can also produce holes.[9] Although the Pt surface is atomically rough in reality, the relative motion of Pt to the SiC surface by the two-axis rotation enables us to assume that the Pt surface is flat.

After flattening, the SiC sample was treated by a post-flattening process with the intention of removing contamination or local oxides. First, it was cleaned with a solution of H_2SO_4(97 wt %):H_2O_2(30 wt %)=4:1 (by volume, 90 °C) for 10 min, Second, it was immersed into concentrated HF solution (50 wt %) for 10 min, which was followed by rinsing with water for 1 min. Finally, the sample was blown dry with pure N_2 gas.

Figure 1(a) shows an atomic force microscopy (AFM) image of the flattened $4H$-SiC(0001) surface. In the inset, an AFM image before flattening is superimposed. The two images in Fig. 1(a) clearly demonstrate that the SiC surface is
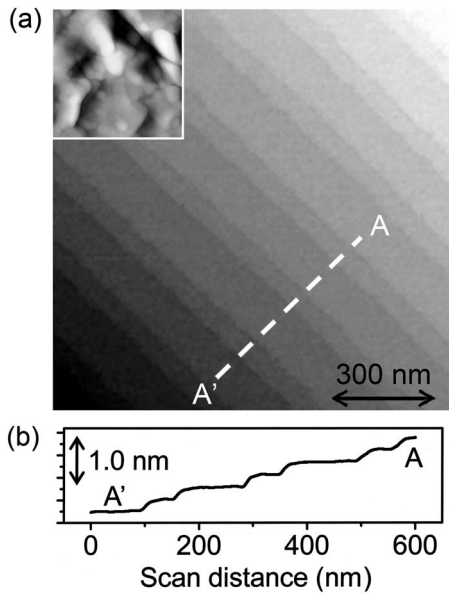
[a)]Electronic mail: arima@prec.eng.osaka-u.ac.jp

FIG. 1. (a) AFM image of flattened 4*H*-SiC(0001) surface. The inset shows an image (1200×1200 nm^2) before flattening in which the peak-to-valley height is 116 nm. (b) Cross-sectional cut along dashed line between *A* and *A'* in (a).

flattened. The flattened terraces in Fig. 1(a) show regularly alternating large and small widths with straight step edges. Figure 1(b) demonstrates that the step height is uniform and 0.25 nm, which corresponds to a single bilayer of 4*H*-SiC(0001). This characteristic terrace width distribution with single-bilayer-height steps, as shown in Fig. 1, can be ascribed to the layer structure of 4*H*-SiC(0001). The 4*H*-SiC(0001) surface has two kinds of terraces (4*H*1 and 4*H*2), depending on the physical relationship with the bilayers below, as shown in Fig. 2. The extra energies required for depositing one new bilayer on the terraces were calculated as follows (in meV per Si–C pair):[13–16]

$$4H1 \text{ terrace:} \quad \Delta U_{\text{growth}}^{4H1} = E_0 + 2.34, \quad (4)$$

$$4H2 \text{ terrace:} \quad \Delta U_{\text{growth}}^{4H2} = E_0 - 6.56. \quad (5)$$

E_0 is the energy of a Si–C pair without the interaction between neighboring bilayers. On the basis of these calculations, energy changes with the desorption of one bilayer are given as follows (in meV per Si–C atoms):

$$4H1 \text{ bilayer:} \quad \Delta U_{\text{etching}}^{4H1} = -\Delta U_{\text{growth}}^{4H2} = -E_0 + 6.56, \quad (6)$$

$$4H2 \text{ bilayer:} \quad \Delta U_{\text{etching}}^{4H2} = -\Delta U_{\text{growth}}^{4H1} = -E_0 - 2.34. \quad (7)$$

Equations (6) and (7) indicate that the 4*H*1 bilayer is more difficult to desorb than the 4*H*2 bilayer. We propose
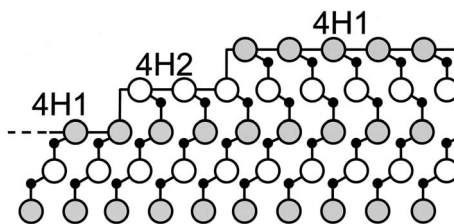

FIG. 2. Schematic drawing of terraces on 4*H*-SiC(0001) surfaces viewed from the [11$\bar{2}$0] direction. Open and shaded circles represent Si atoms at cubic and hexagonal sites, respectively. Closed circles represent C atoms.
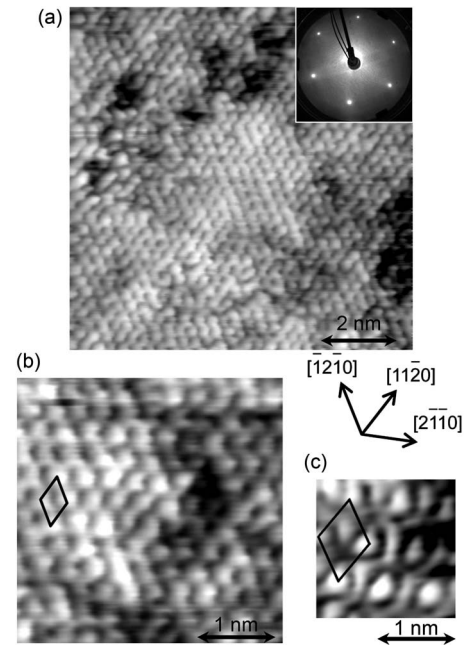

FIG. 3. STM images of flattened 4*H*-SiC(0001) surface. (a) Terrace composed of 1×1 phase. The inset shows a LEED image (70 eV). (b) Magnified image of 1×1 structure. The 1×1 grid is superimposed. (c) Image of 2×2 structure. The 2×2 unit cell is superimposed.

that the wide and narrow areas in Fig. 1(a) correspond to the 4*H*1 and 4*H*2 terraces, respectively. It is likely that the alternating wide and narrow terraces in Fig. 1(a) originate from the rate difference of the chemical reactions in Eqs. (2) and (3) between the 4*H*1 and 4*H*2 terraces.

Figure 3(a) shows a typical scanning tunneling microscopy (STM) image of the flattened 4*H*-SiC(0001) surface. STM observations were performed in UHV (3.5×10^{-8} Pa) with a Pt–Ir tip. It is clear that the bright dots form a large terrace with some atomic-scale defects. The low energy electron diffraction (LEED) image exhibits a sharp and bright 1×1 pattern, as shown in the inset of Fig. 3(a). This indicates that an ordered surface with two-dimensional SiC-bulk periodicity is formed by the flattening process. A closeup image is shown in Fig. 3(b). In Fig. 3(b), the distance between neighboring bright dots is equal to 0.30–0.33 nm along three directions. The crystallographic distance between neighboring outermost Si atoms on an unreconstructed 4*H*-SiC(0001) surface is 0.308 nm, which indicates that a 1×1 structure has formed on the surface shown in Fig. 3(b). The STM image in Fig. 3(b) is in agreement with the 1×1 LEED pattern in the inset of Fig. 3(a). From the distribution of the bright dots, the crystallographic directions are determined, as shown next to Fig. 3(b). Furthermore, local periodic structures with different unit cells were obtained. An example is shown in Fig. 3(c), in which a 2×2 structure has formed. A $\sqrt{3} \times \sqrt{3}$ structure was also observed. Note that these 2×2 and $\sqrt{3} \times \sqrt{3}$ structures exist in a limited area on the order of nm^2, which is why we obtain only 1×1 spots in the LEED image in Fig. 3(a).

Figure 4(a) shows the result of x-ray photoelectron spectroscopy (XPS) for the Si 2*p* core level of the flattened SiC surface. The curve-fitting result in Fig. 4(a) demonstrates that the Si 2*p* spectrum consists of two main components. One is a SiC-bulk component, and the other is a chemically shifted component separated by 0.57 eV. It has been reported that
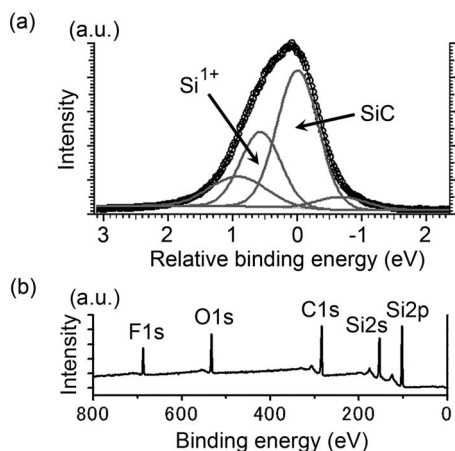
FIG. 4. XPS spectra at the takeoff angle of 20°. (a) Spectrum of Si 2*p* core level. Open circles represent measured data. A deconvolution of the spectrum is also shown. (b) Survey scan.

the second component corresponds to Si^{1+}.[17–19] Figure 4(b) shows a survey scan of the surface. In addition to intense signals from the Si and C atoms, strong peaks from F and O atoms are detected. We assign the Si^{1+} signal in Fig. 4(a) to F- or OH-terminated Si atoms bonded to three C atoms. We confirmed from the F 1*s* and O 1*s* signals that significant amounts of both Si–F and Si–OH bonds exist, respectively. From these XPS spectra, it is concluded that F- and OH-terminated Si atoms coexist on the flattened SiC surface, and they form the 1×1 phase shown in Figs. 3(a) and 3(b). For 4*H*-SiC(0001) surfaces, the underlying Si–C bonds are polarized, because the electronegativity of the C atom (2.5) is larger than that of the Si atom (1.8). Also the outermost Si atoms are positively charged.[20] It is reasonable that negatively charged ions in solutions such as F$^-$ and OH$^-$ are adsorbed on the outermost Si atoms during the electroless chemical reactions shown in Eqs. (1)–(3). In Fig. 4(a), broad chemically shifted components, centered at −0.66 and 0.92 eV, are detected. Although we have not yet assigned these broad peaks, they indicate that the flattened SiC surface is not homogeneous with a perfect F or OH termination, but with a small number of different adspecies. The STM image in Fig. 3(c) supports this idea.

A final point that needs to be addressed is the effect of the postflattening treatments on the surface structures. First, we confirmed that the bimodal surface structure in Fig. 1(a) was formed by the flattening process in HF solution with Pt, and not by the postflattening wet treatments. Second, other XPS spectra showed that the dip into a solution of H$_2$SO$_4$

and H$_2$O$_2$ at 90 °C does not form silicate adlayers (Si^{4+}) but only removes organic impurities on the SiC surface. Furthermore, Si 2*p* signals do not change significantly by the final HF immersion during postflattening cleaning. It is reasonable to conclude that the atomic arrangements discussed in the previous paragraphs are determined by the electroless chemical etching, and not by the postflattening treatments.

[1]S. Fujita, K. Maeda, and S. Hyodo, J. Mater. Sci. Lett. **5**, 450 (1986).
[2]V. V. Afanas'ev, A. Stesmans, M. Bassler, G. Pensl, M. J. Schulz, and C. I. Harris, Appl. Phys. Lett. **68**, 2141 (1996).
[3]U. Starke, Phys. Status Solidi B **202**, 475 (1997).
[4]H. Tsuchida, I. Kamata, and K. Izumi, Jpn. J. Appl. Phys., Part 1 **34**, 6003 (1995).
[5]P. Mårtensson, F. Owman, and L. I. Johansson, Phys. Status Solidi B **202**, 501 (1997).
[6]H. Hara, Y. Sano, H. Mimura, K. Arima, A. Kubota, K. Yagi, and K. Yamauchi, J. Electron. Mater. **35**, L11 (2006).
[7]X. Li and P. W. Bohn, Appl. Phys. Lett. **77**, 2572 (2000).
[8]T. L. Rittenhouse, P. W. Bohn, and I. Adesida, Solid State Commun. **126**, 245 (2003).
[9]S. Yae, Y. Kawamoto, H. Tanaka, N. Fukumuro, and H. Matsuda, Electrochem. Commun. **5**, 632 (2003).
[10]M. Chemla, T. Homma, V. Bertagna, R. Erre, N. Kubo, and T. Osaka, J. Electroanal. Chem. **559**, 111 (2003).
[11]N. Mitsugi and K. Nagai, J. Electrochem. Soc. **151**, G302 (2004).
[12]K. Tsujino and M. Matsumura, Electrochem. Solid-State Lett. **8**, C193 (2005).
[13]V. Heine, C. Cheng, and R. J. Needs, J. Am. Ceram. Soc. **74**, 2630 (1991).
[14]F. R. Chien, S. R. Nutt, W. S. Yoo, T. Kimoto, and H. Matsunami, J. Mater. Res. **9**, 940 (1994).
[15]T. Kimoto, A. Itoh, H. Matsunami, and T. Okano, J. Appl. Phys. **81**, 3494 (1997).
[16]A. Nakajima, H. Yokoya, Y. Furukawa, and H. Yonezu, J. Appl. Phys. **97**, 104919 (2005).
[17]U. Starke, Ch. Bram, P.-R. Steiner, W. Hartner, L. Hammer, K. Heinz, and K. Muller, Appl. Surf. Sci. **89**, 175 (1995).
[18]S. Soubatch, S. E. Saddow, S. P. Rao, W. Y. Lee, M. Konuma, and U. Starke, Mater. Sci. Forum **483–485**, 761 (2005).
[19]N. Sieber, Th. Seyller, R. Graupner, L. Ley, R. Mikalo, P. Hoffmann, D. R. Batchelor, and D. Schmeißer, Appl. Surf. Sci. **184**, 278 (2001).
[20]S. W. King, R. J. Nemanich, and R. F. Davis, J. Electrochem. Soc. **146**, 1910 (1999).